Fast Beamforming for Mobile Satellite Receiver Phased Arrays: Theory and Experiment

Mohammad Fakharzadeh, *Member, IEEE*, S. Hamidreza Jamali, Pedram Mousavi, *Member, IEEE*, and Safieddin Safavi-Naeini, *Member, IEEE*

***Abstract*—The purpose of this paper is to present a robust and fast beamforming algorithm for the low-cost mobile phased array antennas. The proposed beamforming algorithm uses a sequentially perturbation gradient estimation method to update the control voltages of the phase shifters, with the objective of maximizing the received power by the array. This algorithm does not require either the knowledge of phase shifter characteristics or signal Direction-of-Arrival. Moreover, in this paper, the algorithm parameters are derived for the stationary and mobile platform configurations. For the stationary array, it is shown how the proper selection of the beamforming parameters limits the noise effects and increases the array output power. For the mobile array, a condition for the fast convergence is derived and the advantage of using nonuniform step size to update the control voltages is illustrated. When phase shifters suffer from the imbalanced insertion loss the proposed beamforming technique perturbs the phase-conjugate condition to increase the total received power. This algorithm has been implemented with the low-cost microwave components and applied to a Ku-band phased array antenna with 34 sub-arrays. The experimental results verify the broadband performance, and the fast convergence of the algorithm for different platform maneuvers.**

***Index Terms*—Adaptive array, beamforming, mobile phased array antenna, satellite communications, smart antenna.**

I. Introduction

PHASED array antennas have been widely used for satellite communications [1]–[10]. Design and beamforming of the phased arrays with mobile platforms such as airborne [2], shipboard [4], [5] or vehicular platforms [7]–[9] are more delicate and challenging compared to the stationary arrays.

When sufficient information of the source (target) and array is available, there are optimum methods to find the array (phase-shifter) weights which minimize the least mean square error [12]. Such methods are based on inverting the correlation matrix of the received array signals. To find this matrix one must have access to all received signals (in base-band); hence, for each element an individual receiver chain (mixer, IF, decoder,analog to digital converter (ADC), etc.) is required [13]. Furthermore, a reference signal is needed to estimate the error. If the received array signal and noise are jointly ergodic processes, the array correlation matrix is estimated based on calculating the time average of the received signals, which is a time consuming process. Thus, adaptive methods have been used for beamforming to save time [14], [15]. The drawbacks of the optimum and adaptive beamforming algorithms developed so far, can be summarized as:

1) Measuring array correlation matrix is costly requiring N-channel receivers. Estimating this matrix is time consuming and imprecise.
2) If signal Direction of Arrival (DOA) is not known or accurately estimated, calibration errors degrade the beamforming performance seriously [16]. DOA estimation methods such as MUSIC and ESPRIT are complex, lengthy, and sensitive to modeling errors [17].
3) The phase-voltage characteristics of the phase shifters are not accurately predictable and controllable. They are device-dependent and may change with the environmental conditions [9].
4) Platform motions affect the estimated correlation matrix significantly. Even a small relative displacement of the source during the time required for correlation estimation causes a significant error and gain drop [18].

When a combined signal from all antennas is the only available information (single-receiver array antenna), beamforming problem becomes more complicated. Most of the beamforming methods minimize the mean received power while maintaining a fixed beam in a desired direction. Such methods place nulls in antenna patterns in the interference directions [19]–[22], but beamforming for mobile satellite communications, is not an interference-limited problem. In this case beam-agility, fast convergence, robustness, and low-cost implementation are the high priority tasks that must be accomplished by the algorithm.

The main purpose of this paper is to present a robust and fast beamforming algorithm for low-cost mobile phased arrays. The proposed algorithm does not depend on the knowledge of signal DOA. Moreover, it adjusts the control voltages of the phase shifters directly, despite other methods that update the phases. The only available input is a feedback from the array output power. It is shown, both theoretically and experimentally, that the proposed algorithm can compensate for the hardware errors and imperfections of the low-cost components used in the system.

The organization of the paper is as follows. Section II presents the formulation of the proposed algorithm. In Sections III and

Manuscript received June 12, 2008; revised November 20, 2008. Current version published June 03, 2009. This work was supported by the NSERC of Canada, RIM, OCE and Intelwaves Technologies Ltd.

M. Fakharzadeh and S. Safavi-Naeini are with the Department of Electrical and Computer Engineering, University of Waterloo, Waterloo, ON N2L3G1, Canada (e-mail: mfakharz@maxwell.uwaterloo.ca).

S.H. Jamali is with Intelwaves Technologies, Waterloo, ON, Canada and also with the Electrical Engineering Department, Tehran University, Tehran, Iran.

P. Mousavi is with Intelwaves Technologies, Waterloo, ON, Canada (e-mail: pmousavi@intelwaves.com).

Color versions of one or more of the figures in this paper are available online at http://ieeexplore.ieee.org.

Digital Object Identifier 10.1109/TAP.2009.2019911

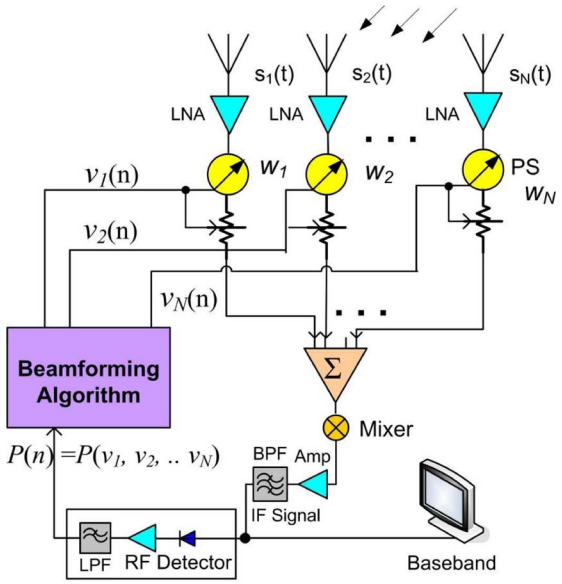

Fig. 1. Block-diagram of a single-channel receiver phased array antenna.

IV the effects of noise and mobility on determining the algorithm parameters are discussed. Section V illustrates an important property of this algorithm named non-coherent beamforming. Section VI presents the experimental results, and finally, Section VII concludes this paper.

II. Zero-Knowledge Beamforming

High-gain antennas used for satellite communications posses narrow beams and low sidelobe levels. Thus, unlike the broad-beam antennas used in cellular networks, the sharp spatial filtering of the satellite receiver antenna attenuates the undesired out-of-beam signals significantly. Hence, beamforming for a satellite receiver array is not an interference or multipath-limited problem. Instead, the objective is to maximize the received power or signal to noise ratio.

We define *Zero-knowledge* beamforming as a constrained nonlinear optimization problem whose objective is to maximize the received power, without knowing the signal DOA. Usually, knowledge of DOA helps calculating proper initial conditions for beamforming, while Zero-knowledge beamforming does not depend on a specific initial condition. Despite some similarities in the form and formulation, this method is intrinsically different from the unconstrained LMS-based algorithms [14]. Unlike those algorithms, here the signal DOA and the phase-voltage characteristics of the phase shifters are unknown, and the algorithm directly adjusts the control voltages of the phase shifters to increase the received power. Fig. 1 shows the block diagram of a single receiver phased array antenna with N radiating elements. After being amplified by Low Noise Amplifiers (LNAs) the received signals, $[s_1(t) \quad s_2(t) \ldots s_N(t)]$, pass through the lossy phase shifters whose control voltages, $[v_1(t) \quad v_2(t) \ldots v_N(t)]$, are adjusted by the beamforming unit. All phase-shifted signals are combined by a power combiner, denoted by Σ, and down-converted to an Intermediate Frequency (IF) by a mixer. The IF signal is amplified and filtered. A fraction of the IF signal enters a detector which measures the instantaneous received power to provide the only available input for beamforming unit.

A. Formulation of the Optimization Problem

The received power by the phased array is given by

$$P = \mathbf{w}^H \mathbf{R} \mathbf{w} \tag{1}$$

where $\mathbf{w} = [w_1 \quad w_2 \quad \ldots w_N]^T$ denotes the phase shifter weights, ^{H} is the Hermitian operator and $\mathbf{R}$ is the correlation (covariance) matrix of the received signals. For the interference-free problems the signal to noise ratio is given by

$$\rho = \sigma_n^{-2} \frac{\mathbf{w}^H \mathbf{R}_S \mathbf{w}}{\mathbf{w}^H \mathbf{w}} \tag{2}$$

where $\mathbf{R}_S = E\left\{\mathbf{x}_S(t)\mathbf{x}_S^H(t)\right\}$ is the correlation matrix of the source signal vector $\mathbf{x}_S(t)$. To find the optimum array weights, which maximize ρ in (2), the correlation matrix, $\mathbf{R}_S$ must be calculated or estimated in advance. For constrained LMS algorithms, the steering vector, $\mathbf{s}_0$, must be known as well. Steering vector gives the array weights required to point the beam to the source direction. So to calculate s_0 the signal DOA and phase shifter characteristics must be known accurately. In this case the well-known sample matrix inversion method (SMI) gives the following optimal weights:

$$\mathbf{w}_{opt} = \frac{\mathbf{R}^{-1}\mathbf{s}_0}{\mathbf{s}_0^H \mathbf{R}^{-1} \mathbf{s}_0}. \tag{3}$$

The received SNR for a uniform linear array is then

$$\rho = \frac{\sum_{k=1}^{N} \sum_{l=1}^{N} w_l w_k^* e^{j(l-k)u}}{\sigma_n^2 \sum_{k=1}^{N} |w_k|^2}. \tag{4}$$

The unconstrained solution which maximizes (4), known as *phase-conjugate* relation, is

$$w_k^* = g_0 e^{jku} \quad \forall\, k \tag{5}$$

where g_0 is a constant.

B. Voltage-Controlled Beamforming

In practice, both phase and amplitude of the phase shifters vary with the control voltages [23]. Thus, each array weight w_k can be denoted by a complex number

$$w_k(v_k) = f(v_k) \cdot \exp[j\psi(v_k)]. \tag{6}$$

whose amplitude (f) and phase (ψ) depend on the control voltage. Both f and ψ functions do not have exact mathematical expressions and are found via measurements. Fig. 2 shows the *general behavior* of the low-cost analog phase shifters [23]. The phase function, $\psi(v)$, shown in Fig. 2(a) has a monotonic behavior and can be approximated by a line. However, the amplitude function $f(v)$ shows nonlinear behavior and must be

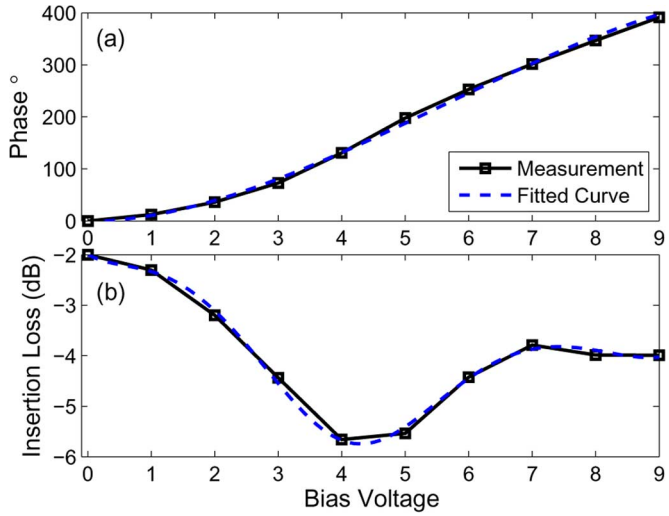

Fig. 2. Measured characteristics of analog phase-shifters [23], at $f = 12.45$ GHz. The dashed lines show the fitted polynomials. (a) Phase-shift versus voltage, (b) insertion loss versus voltage.

approximated by a high order polynomial $(n \geq 6)$. For voltage controlled phase shifters the signal to noise ratio in (4) is given by

$$\rho = \frac{\sum_{l,k=1}^{N} f(v_l) f(v_k) e^{j[\psi(v_l)-\psi(v_k)]} e^{j(l-k)u}}{\sigma_n^2 \sum_{k=1}^{N} f(v_k)^2} \tag{7}$$

which is in general a nonlinear function of the control voltages. So the beamforming problem when practical phase shifters are used can be stated as a nonlinear maximization problem

$$\begin{aligned} \text{maximize} \quad & P = \mathbf{w}^H \mathbf{R} \mathbf{w} \text{ or } \rho = \sigma_n^{-2} \frac{\mathbf{w}^H \mathbf{R}_S \mathbf{w}}{\mathbf{w}^H \mathbf{w}} \\ \text{subject to:} \quad & w_k = f(v_k) \cdot \exp[j\psi(v_k)] \quad \forall\, k. \end{aligned} \tag{8}$$

Solving this nonlinear problem with ordinary optimization methods is not practical in real-time. Thus, in the following, we propose an iterative approach to find the control voltages which maximize the received power.

C. Beamforming Algorithm

As long as the phase-voltage relation of the phase shifter is monotonic and can be modeled by a linear function, the received power can be well approximated by a quadratic function around the quiescent point [19]. It is well known that the optimum solution for maximizing (or minimizing) a quadratic function can be found via an iterative process. So, we propose an iterative gradient estimation method to update the control voltages.

1) Update Equation: Let $\mathbf{v}(n) = [v_1(n) \quad v_2(n) \quad \dots \quad v_N(n)]$ denote the control voltages of N phase shifters at time n. The new set of the control voltages $\mathbf{v}(n+1)$ is given by

$$\mathbf{v}(n+1) = \mathbf{v}(n) + 2\mu \nabla_{\mathbf{v}} P(n) \tag{9}$$

where μ is an internal algorithm parameter called *step-size*, and $\nabla_{\mathbf{v}} P(n)$ is the gradient of power with respect to $\mathbf{v}(n)$. Since the exact calculation of the gradient is not practical, it is replaced by an estimated vector, such as

$$\nabla_{\mathbf{v}} P(n) \simeq [\hat{g_1}(n) \quad \hat{g_2}(n) \dots \hat{g_N}(n)] \tag{10}$$

where each component $\hat{g_k}(n)$ is the approximate partial derivative of $P(n)$ w.r.t. $v_k(n)$.

2) Gradient Approximation Methods: Sequential two-sided approximation method requires two different power measurements to determine the centered finite-difference approximation of each gradient component, thus

$$\hat{g_k}(n) = \frac{P[\dots, v_k(n)+\delta, \dots] - P[\dots, v_k(n)-\delta, \dots]}{2\delta} \tag{11}$$

where δ called *perturbation* is an internal algorithm parameter. This method has less power fluctuations at steady state compared to other gradient estimation methods [9]. The criteria for selecting the algorithm parameters will be discussed in Sections III and IV.

III. Controlling the Noise Effect on Gradient Estimation

Due to noise, multipath, interference from other active sources, and mobility of the platform the received power has a spread spectrum, and accordingly fluctuations in time domain. Consider a zero mean Gaussian noise, $n_m(t)$, called the *measurement noise*, with variance σ^2, added to the received power. The noisy estimate of the gradient in (11) is then

$$\begin{aligned} \widetilde{g_k} &= \frac{[P(v_k+\delta)+n_{m1}] - [P(v_k-\delta)+n_{m2}]}{2\delta} \\ &= \frac{P(v_k+\delta) - P(v_k-\delta)}{2\delta} + \frac{n_{m1}-n_{m2}}{2\delta} = \hat{g_i} + \widetilde{n}_g(t) \end{aligned} \tag{12}$$

where n_{m1} and n_{m2} are two samples of $n_m(t)$. Additionally, $\widetilde{n}_g(t)$ called the gradient estimation noise is a zero mean Gaussian noise with the variance of $\sigma^2/2\delta^2$. Equation (11) proposes that by reducing perturbation, the accuracy of gradient estimation increases. However, for small values of δ, i.e., $\delta < \sigma/\sqrt{2}$, the gradient estimation noise dominates the measurement noise $(E\{\widetilde{n}_g^* \widetilde{n}_g\} > E\{n_m^* n_m\})$. Thus, small values of δ must be avoided. Nonetheless, further increase of δ deteriorates the gradient approximation in (11). If we replace $\hat{g_k}$ in (10) with $\widetilde{g_k}$ given in (12), the updated voltage becomes noisy. The noisy updated voltage, $\widetilde{v_k}(n+1)$, is thus

$$\widetilde{v_k}(n+1) = v_k(n+1) + n_u(t). \tag{13}$$

In (13), $\widetilde{v_k}(n+1)$ and $v_k(n+1)$ differ in a noise term denoted by $n_u(t)$ equal to $2\mu\widetilde{n}_g(t)$. Added to the phase shifter control voltage, this noise affects the received power level. Hence, the noisy estimated gradient in (12) must be modified to

$$\widetilde{g_k} = \frac{P(v_k+\delta+n_{u1}) - P(v_k-\delta+n_{u2})}{2\delta} + \widetilde{n}_g(t)$$

where n_{u1} and n_{u2} are two samples of $n_u(t)$. Writing the Taylor series expansion for the received power, we have

$$P(v_k \pm \delta + n_u) = P(v_k) + P'(v_k)(\pm\delta + n_u) + \frac{1}{2!}P''(v_k)(\pm\delta + n_u)^2 + \cdots$$

Thus, the noisy estimated gradient $\widetilde{g_k}$ is evaluated as

$$\widetilde{g_k} = \widetilde{n}_g(t) + P'(v_k)\left[1 + \frac{n_1 - n_2}{2\delta}\right] + \frac{1}{4}P''(v_k)\left[n_1 - n_2 + \frac{n_1^2 + n_2^2}{2}\right] + \cdots$$

It is a reasonable assumption that the second derivative diminishes as the algorithm reaches its steady state, so the second and higher order terms in the previous equation can be ignored. The noisy estimated gradient is thus

$$\widetilde{g_k} \simeq P'(v_k)\left[1 + \widetilde{n}_v\right] + \widetilde{n}_g(t) \tag{14}$$

where $\widetilde{n}_v$ denotes a zero mean Gaussian noise with the variance of $(\mu\sigma/\delta^2)^2$. For a fixed σ/δ^2 ratio, decreasing μ diminishes the effect of the voltage updating noise. Simulation results showing the effects of different values of μ and δ on the convergence and steady state behavior of the received power are given in [24] and [25].

IV. Beamforming in Motion

The received power by a linear N-element array, when the source is located at $\theta(n)$ relative to array normal, is given by

$$P(n) = \left|\sum_{k=1}^{N} \exp\left[-j\psi_k(n) + jk_0x_k\sin\theta(n)\right]\right|^2 \tag{15}$$

where x_k and ψ_k denote the position and the applied phase shift to the kth element, respectively. For a stationary array, $(\theta(n) = \theta_0)$, the beamforming algorithm adjusts all $\psi_k(n)$ coefficients to maximize $P(n)$. It may take a few iterations to reach the steady states, when $P(n)$ converges to the proximity of N^2 and the phase-shift variations become zero, i.e.,

$$\psi_k(n) \simeq k_0x_k\sin\theta_0 \quad \forall\, k. \tag{16}$$

Zero-knowledge algorithm calculates $\psi_k(n)$ weights based on the power measurements at the previous time instant $n-1$. Thus, for a mobile array, where $\theta(n)$ is varying, the algorithm always lags the target movements. Consequently, the phase differences differ from zero. This causes a power level drop. A *fast beamforming* algorithm minimizes this level drop. The convergence time or the execution time of the algorithm, ΔT must be adequately short to track the fast target movements without a significant power drop. In this case $\theta(n)$ can be approximated by a linear function of the angular velocity at $n-1$

$$\theta(n) \simeq \theta(n-1) + \dot{\theta}(n-1)\Delta T. \tag{17}$$

If rate sensors with high sampling rates were available, one could estimate the target location at the next iteration and adjust the weights accordingly, but there are two major problems compelling us to look for a fast beamforming technique.

1) The convergence/execution time of the algorithm is several times faster then the sampling interval of the low-cost rate sensors, thus delay in beamforming causes a large power drop leading to missing of the target.
2) Zero-knowledge beamforming is a feedback aided method which assumes no *a priori* knowledge of the phase shifters, so the phases cannot be adjusted in advance to steer the beam to the predicted position.

A. Fast Beamforming Condition

To figure out how beamforming parameters must be chosen for fast convergence, consider a uniform N-element linear phased array. The necessary condition for fast convergence in a mobile scenario is given by

$$\left|\psi_k(n+1) - k_0x_k\sin\theta(n)\right| \ll 1. \tag{18}$$

This condition implies that the array weights applied at iteration $n+1$ must equalize the received signal phases at iteration n. If (18) is not satisfied the phase differences accumulate, and consequently the total received power decreases due to the destructive interference. Assume array wights are directly updated based on gradient estimation

$$\psi_k(n+1) = \psi_k(n) + 2\mu_\psi\hat{g_k}(n). \tag{19}$$

Two power measurements are required to estimate the kth component of the gradient vector, $\hat{g_k}(n)$. In Appendix, it is shown that for a linear array $\hat{g_k}(n)$ can be expressed as

$$\hat{g_k}(n) = 2\frac{\sin\delta_\psi}{\delta_\psi}\sin\left[\left(\frac{N+1}{2} - k\right)\gamma(n)\right]\frac{\sin\left[\frac{N\gamma(n)}{2}\right]}{\sin\left[\frac{\gamma(n)}{2}\right]} \tag{20}$$

$$\gamma(n) = k_0d[\sin\theta(n) - \sin\theta(n-1)]. \tag{21}$$

B. Nonuniform Step-Size

To satisfy the fast convergence condition for a linear array given in (18), the beamforming algorithm at time $n+1$ must compensate for the angular motions between $n-1$ and n, so

$$\psi_k(n+1) - \psi_k(n) = k_0x_k[\sin\theta(n) - \sin\theta(n-1)]. \tag{22}$$

The left-side of (22) is the difference in the applied phase-shifts at $n+$ and n. From (19) it is concluded that

$$\psi_k(n+1) - \psi_k(n) = 2\mu_\psi\hat{g_k}(n). \tag{23}$$

Equating the right-sides of (22) and (23) we have

$$\mu_\psi\left[2\hat{g_k}(n)\right] = x_k\left\{k_0[\sin\theta(n) - \sin\theta(n-1)]\right\}. \tag{24}$$

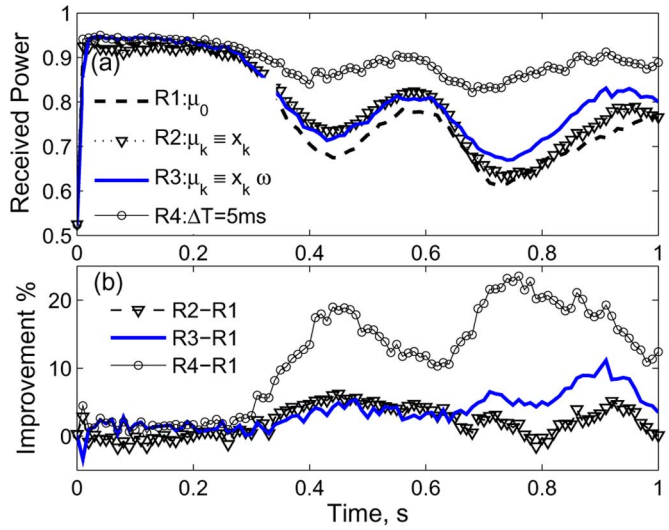

Fig. 3. Comparison of beamforming with different step-size options for a mobile linear array. Each curve represents the mean value of 100 runs of the algorithm. R1: uniform time-invariant step-size $T_s = 10\,\mathrm{ms}$, R2: nonuniform time-invariant step-size $T_s = 10\,\mathrm{ms}$, R3: nonuniform time-variant $T_s = 10\,\mathrm{ms}$, and R4: nonuniform time-variant step-size with $T_s = 5\,\mathrm{ms}$ (a) Received power versus time, (b) improvement percentage.

Replacing $\hat{g_k}(n)$ with (20) it is found that the step-size μ_ψ in (24) cannot have a constant value for all elements. It must be proportional to the element location x_k, thus

$$\mu_k = \left[\frac{\delta_\psi}{4\sin\delta_\psi}\frac{\sin\left(\frac{\gamma(n)}{2}\right)}{\sin\left[\frac{N\gamma(n)}{2}\right]}\right]\frac{\frac{\gamma(n)x_k}{d}}{\sin\left[\left(\frac{N+1}{2}-k\right)\gamma(n)\right]}. \quad (25)$$

For relatively fast beamforming $\gamma(n)$ depends on the angular velocity and the execution time of the algorithm

$$\gamma(n) = k_0 d\Delta T\dot{\theta}(n)\cos\theta(n-1). \quad (26)$$

Hence, the following conclusions are extracted for a mobile array:

- μ_k depends on the element location, x_k;
- μ_k increases with the angular speed of the array;
- μ_k decreases if the beamforming speed increases;
- μ_k increases with the phase perturbation δ_ψ (because $\sin(\delta_\psi) \leq \delta_\psi$).

In the stationary situation when $\dot{\theta} \to 0$ the step-size (μ_k) becomes independent of the element locations. We refer to this special case as uniform step-size situation $(\mu_k = \mu_0,\ \forall\, k)$.

To investigate the merit of employing nonuniform step-sizes for beamforming, we assume a mobile linear array of 12 elements with 5λ spacing. The spacing is fairly large, because in satellite communications each phased array element must be a high-gain sub-array with a size of several wavelengths to meet the gain requirements. The array platform is rotated with a relative angular velocity of $\dot{\theta} = 40\sin(2\pi/5t)^\circ/s$. This angular velocity models an accelerating fast maneuver during a short time period. At $t = 0$ the array is located at $\theta(0) = 100^\circ$. First we assume the execution time of the algorithm (ΔT) is 10 ms. The curve R1 in Fig. 3(a) (the dashed line) shows the mean value of the received power for 100 runs of beamforming with uniform step-size. When the angular speed is relatively low $(0 \leq t \leq 0.25\ \mathrm{s})$, the beamforming algorithm converges to 92% of the maximum power. However, as the time passes the power level drops to below 65%. In the curve R2 step-size depends on element location. The mean power level improves by 3% compared to R1. In the curve R3 (the solid line) step-size depends on both element position and angular speed of platform. The overall performance of R3 is 5.1% better than that of R1. The curve R4 is similar to R3 but the algorithm is two times faster $(\Delta T = 5\,\mathrm{ms})$. In this case the average power level is 16.4% better than R1. These simulations reveal that using nonuniform step-size improves the beamforming performance of mobile linear arrays. If the angular velocity of the array platform is known the improvement is further enhanced. Moreover, increasing the beamforming speed has a significant effect, but it requires a revision in the processor and hardware design. Thus, use of nonuniform step-size is the low-cost solution to obtain a better performance.

V. Non-Coherent Beamforming

Considering the imbalanced loss of phase shifters [Fig. 2(b)], in this section we show zero-knowledge beamforming perturbs phase-coherency to increase the received power.

Based on the maximum array gain theorem, when all array elements are identical, coherent beamforming, see (5), gives the maximum gain (power). In coherent beamforming each array weight is proportional to the complex conjugate of its corresponding received signal [26]. Let $\phi_k(n)$ denote the phase of the received signal by the kth element, then the total received power through *coherent* beamforming $(\psi_k = \phi_k)$ is

$$\begin{aligned} P_{Coh}(n) &\equiv P\left(\psi_1(n) = \phi_1(n), \ldots, \psi_N(n) = \phi_N(n)\right) \\ &= \left|\sum_{k=1}^{N} f(\phi_k(n))\right|^2 \end{aligned} \quad (27)$$

where $f()$ is the insertion loss of phase shifter defined in (6). Provided that all phase shifters are lossless, $(f(\phi_k) = 1)$ the coherent power is equal to N^2, which is the maximum achievable power. Otherwise, it is not guaranteed that coherent beamforming yields the maximum power. Suppose the coherency condition is violated. Thus, the applied phase shift to each element includes an additive non-coherent phase, denoted by $\xi_k(n)$, i.e.,

$$\psi_k(n) = \phi_k(n) + \xi_k(n). \quad (28)$$

Thus, the non-coherent received power is defined as

$$\begin{aligned} P_{Non}(n) &\equiv P(\phi_1(n) + \xi_1(n), \ldots, \phi_N(n) + \xi_N(n)) \\ &= \left|\sum_{k=1}^{N} f(\phi_k(n) + \xi_k(n))e^{-j\xi_k(n)}\right|^2. \end{aligned} \quad (29)$$

Fig. 4 compares the results of coherent and non-coherent beamforming for the 17-element array, discussed in Section VI, when the satellite is located at $(\theta, \phi) = (18^\circ, 18^\circ)$ and the array is stationary. First, the coherent phase shifts were calculated and the phase shifters were adjusted to generate these values. The received power after applying these initial values was 53% of the maximum expected power. Next, Zero-knowledge

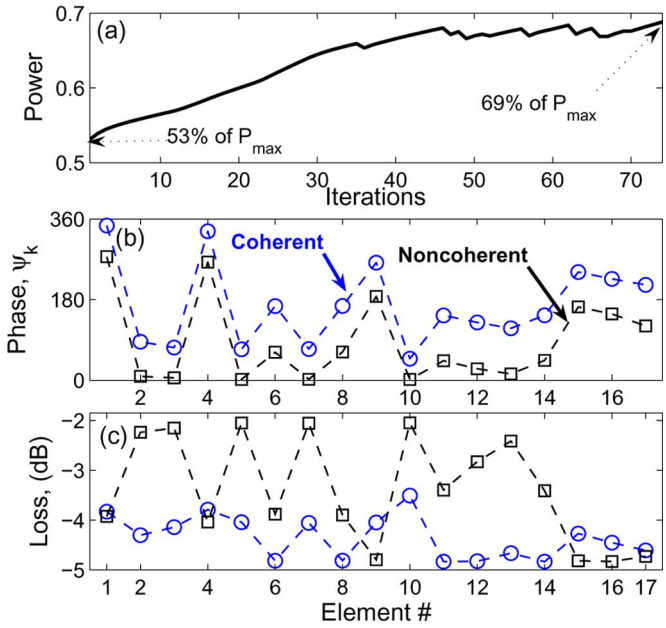

Fig. 4. Comparison of the coherent and non-coherent beamforming for the 17-element phased array when the satellite is at $(\theta, \phi) = (18^\circ, 18^\circ)$ relative to normal. (a) Learning curve of the normalized power, (b) coherent and non-coherent phase shifts, and (c) amplitude of the array weights.

beamforming algorithm was run for 75 iterations to update the control voltages of the phase shifters. All phase shifters were identical to the one shown in Fig. 2. The algorithm parameters were set to $\mu = 0.1$, $\delta = 0.3$ and $SNR = 32$ dB. This is the SNR over a narrow bandwidth (at the baseband) after power detector in Fig. 1. Fig. 4(a) shows that after 75 iterations of beamforming the received power has increased by 16%. Fig. 4(b) and (c) compares the phase and insertion loss of all phase shifters before and after beamforming. It is evident that the insertion loss has significantly reduced after beamforming, with the price of perturbing phase-coherency. Hence, the proposed beamforming algorithm is not a coherent method, so it can increase the total received power when phase shifters suffer from the nonuniform insertion loss.

VI. Experimental Results

Fig. 5 shows the configuration of the stair-planar single-receiver phased array system used for the experiments. This low-profile array antenna $(h < 6$ cm$)$ consists of ten rows. The five right rows support left hand circular polarization (LHCP) while the five left rows support right hand circular polarization (RHCP). Each row includes three or four radiating modules in the form of 2×8 and 2×16 microstrip sub-arrays. There are totally 17 sub-arrays for each polarization directly connected to LNAs, which three of them are 2×8 and the rest are 2×16 sub-arrays. Thus, 496 microstrip elements are used for each polarization. The sub-arrays are mounted on array carriers which can mechanically rotate from 20° to 70° in elevation plane and from 0° to 360° in azimuth plane using two stepper motors. A single receiver architecture similar to Fig. 1 is used for this phased array system. All electronic parts are integrated in the

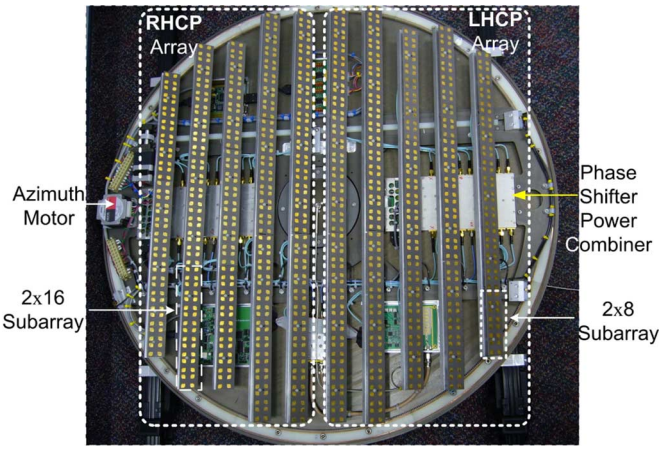

Fig. 5. Developed phased array system with 34 sub-arrays.

TABLE I
Low Profile Phased Array System Parameters

Frequency	12.2-12.7 GHz
Polarization	Dual Circular
Array Gain	31.5 dBi (per polarization)
Sub-Array Size	11.2, 22.3 cm
Sub-array Gain	17.8, 19.5 dBi
Maximum Tracking Speed	$60^\circ s^{-1}$ (Azimuth)
System Dimension	Height: 6cm, Diameter: 86cm

rotating part of the mechanical platform. Some of the system parameters are summarized in Table I. More details of the system design and phased array components can be found in [27].

A. Spectral Measurements

The carrier frequency of DBS satellites in North America ranges from 12.2 to 12.7 GHz resulting in a bandwidth of 500 MHz, or a fractional bandwidth $(\Delta f / f_0)$ of 4% around the center RF frequency. Thus an important test is to evaluate the broadband performance of the proposed beamforming algorithm.

To investigate how the proper selection of the beamforming parameters affects the spectral response of the array, two tests were designed. Initially, the best location of the satellite providing the highest received power was found. In the first test, the algorithm parameters were set to $\mu = 0.1$ and $\delta = 0.5$. Based on the discussions in Section III and [24], this set of parameters causes a slow convergence. Agilent E4405B spectrum analyzer was used to measure the spectral response of the array. For each spectral measurement, the average of 200 successive frames were taken to smooth the instantaneous power fluctuations. The three curves in Fig. 6(a) respectively show the IF spectrum of the received signal before beamforming I_0, after the first iteration I_1, and after 10 iterations I_{10} of beamforming. Five satellite transponders are distinguishable in this figure. In the second test, parameters were set to $\mu = 0.4$ and $\delta = 1$ for fast convergence. Fig. 6(b) demonstrates I_0, I_1 and I_{10} for this test. The reference level, frequency span and scales of both figures are the same and respectively equal to -51.66 dBm, 150 MHz, and (15 MHz, 1 dBm). In Fig. 6(b), a large gap between

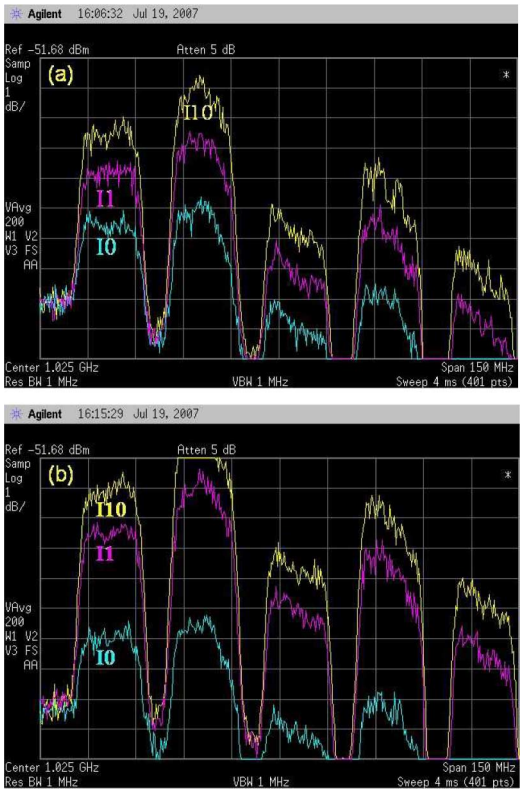

Fig. 6. IF Spectrum of the received satellite signal for two different set of algorithm parameters.

I_0 and I_1 is observed indicating that even one iteration of the algorithm increases the received power significantly. Furthermore, the curve I_{10} for the second test is between 1.2 to 2.5 dB higher than that of the first test. These spectral measurements indicate the satisfactory broadband performance of the algorithm. Furthermore, they illustrate that the proper selection of μ and δ, results in a faster convergence.

B. Merit of Nonuniform Step-Size

In this experiment the results of beamforming tests with uniform and nonuniform step-sizes are compared. Both tests started with the same initial conditions, i.e., $\mathbf{v}_0 = 6$ V. The uniform step-size was fixed at $\mu = 0.25$. The nonuniform step-size was varied proportional to the element location such that the mean value of step-sizes remained equal to 0.25. If r_k denotes the location of element k, then μ_k is calculated using the following:

$$\mu_k = 0.126 + 0.45 r_k \tag{30}$$

$$r_k = \sqrt{x_k^2 + y_k^2} \text{ and } \overline{[\mu_k]} = 0.25. \tag{31}$$

For each case the beamforming algorithm was run for 50 times. Fig. 7 depicts the mean values of the normalized received power. The average received power after 50 iterations is 6% higher when the nonuniform step-size is used.

C. Three Platform Maneuvers

To study the Zero-knowledge beamforming behavior for a mobile platform, rate sensors were mounted on a van vehicle. Road test measurements were performed for three maneuvers:

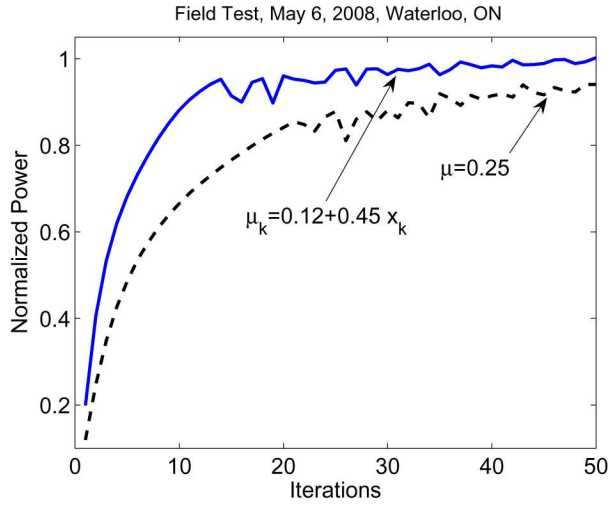

Fig. 7. Experimental results for uniform and nonuniform step-sizes.

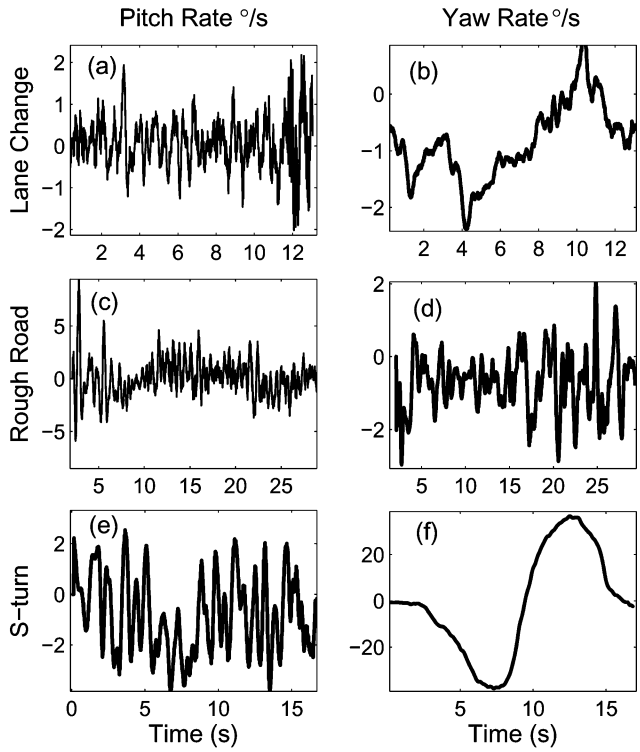

Fig. 8. Measured pitch and yaw rates of three vehicle maneuvers. (a)–(b) Two lane changes, (c)–(d) driving on a rough road, and (e)–(f) making a sharp S-turn.

1) two successive lane changes; 2) driving on rough road; and 3) making a sharp S-turn. Fig. 8 shows the pitch rate and yaw rate of the van for these maneuvers. The sampling rate of the rate sensors in all tests was 100 Hz. The mechanical servo-system was controlled by a direction finding algorithm to maintain the satellite in the array field of view. This algorithm compares the control voltages updated by the Zero-knowledge beamforming with a set of pre-default values to find the relative direction of the satellite [24], [28]. The beamforming algorithm was executed for each maneuver. The execution time of one beamforming iteration was set to 10 ms. The SNR after power detector (with 8-point Hamming digital filtering) was estimated to be 31 dB.

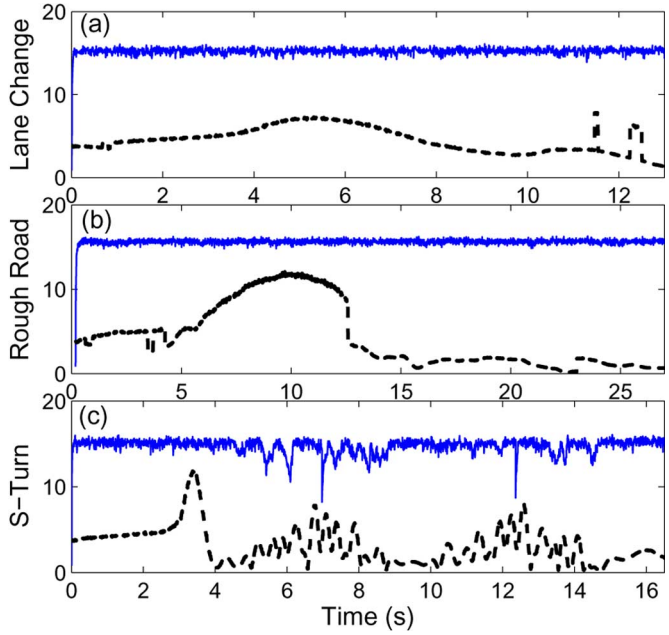

Fig. 9. Beamforming results for three maneuvers. The vertical axis shows the received power by the 17-element phased array. The dashed lines show the received power with a fixed beam normal to array.

Fig. 9 compares the received power level by the 17-element phased array for each maneuver with and without beamforming. For double lane change and driving on rough surface the performance of the algorithm was satisfactory, because the signal level never dropped during these maneuvers. However, for the sharp S-turn maneuver the received signal faded several times and even dropped to below 52% of the maximum value, but after a short fading period the beamforming algorithm could recover the power level. Comparing Figs. 8(c) and 9(c) one can find that the maximum fading occurs at $t = 6.97\,\mathrm{s}$ and $t = 12.36\,\mathrm{s}$, when the yaw rate reaches its extreme points. In this case the algorithm must be executed faster to achieve a better performance.

VII. Conclusion

Zero-knowledge beamforming algorithm adjusts the control voltages of the phase shifters based on the instantaneous power measurements. The objective of this algorithm is to increase or even maximize the total received power. Since this algorithm does not depend on the phase shifter characteristics and satellite DOA, it eliminates an expensive laborious calibration procedure. Furthermore, it can be implemented with low-cost components.

For a stationary scenario, use of a small step size with a fairly large perturbation diminishes the noise impairments, while in a mobile scenario the fast convergence condition relates step-size to perturbation and predicts that for each element an individual step-size proportional to the relative location of that elements is required. Simulation and experimental results prove that a nonuniform step-size results in a higher power level and faster convergence. The proposed beamforming technique overcomes an intrinsic drawback of the commercial analog phase shifters, i.e., the imbalanced insertion loss. It perturbs the phase-coherency to reduce the insertion loss at the quiescent point of the phase shifters. Furthermore, three different maneuvers were devised to test the performance of the algorithm for a mobile platform. For the execution time of 10 ms per iteration, the algorithm was able to track satellite as long as the absolute angular speed was below $20^{\circ}\mathrm{s}^{-1}$.

The Zero-knowledge beamforming is a feedback aided method so it can adapt to ambient changes and calibrate itself. The functionality of this algorithm in different weather conditions has been proved by hundreds of field tests at different times of the year.

Appendix
Derivation of (20)

The total received power in (15) depends on the array position and array weights. For a fast beamforming the array movement during gradient estimation is negligible. The kth component of the estimated gradient vector in (19), i.e., $\hat{g}_k(n)$, is given by

$$\hat{g}_k(n) = \frac{P(\psi_k(n) + \delta_\psi) - P(\psi_k(n) - \delta_\psi)}{2\delta_\psi} \tag{32}$$

where δ_ψ is the perturbation in phase applied to estimate the gradient. The measured (received) power for gradient estimation can be expressed as

$$P(\psi_k \pm \delta_\psi) = |U_\pm + M|^2 \tag{33}$$

where

$$U_\pm = \exp(\mp j\delta_\psi) \cdot \exp[-j\psi_k(n) + jk_0 x_k \sin\theta(n)] \tag{34}$$

and

$$M = \sum_{m \neq k}^{N} \exp[-j\psi_m(n) + jk_0 x_m \sin\theta(n)]. \tag{35}$$

So $P(\psi_k \pm \delta_\psi)$ is equal to

$$P(\psi_k \pm \delta_\psi) = (U_\pm + M) \cdot (U_\pm^* + M^*). \tag{36}$$

Substituting (36) in (32), after further simplification $\hat{g}_k(n)$ is calculated as

$$\begin{aligned}\hat{g}_k(n) &= \frac{MU_+^* + M^*U_+ - MU_-^* - M^*U_-}{2\delta_\psi} \\ &= \frac{M(U_+^* - U_-^*) + M^*(U_+ - U_-)}{2\delta_\psi}.\end{aligned} \tag{37}$$

Using (34) the above expression can be simplified to

$$\hat{g}_k(n) = \frac{2\sin(\delta_\psi)}{\delta_\psi} \Im[X] \tag{38}$$

where $\Im[X]$ denotes the imaginary part of X defined as

$$X = M \exp[j\psi_k(n) - jk_0 x_k \sin\theta(n)]. \tag{39}$$

The fast convergence condition, given in (18), necessitates that $\psi_m(n) \approx k_0 x_m \sin\theta(n-1)$, so

$$\begin{aligned}&\exp[-j\psi_m(n) + jk_0 x_m \sin\theta(n)] \\ &\qquad \approx \exp[jk_0 x_m (\sin\theta(n) - \sin\theta(n-1))].\end{aligned} \tag{40}$$

The location of the kth element in a linear array is given by

$$x_k = \left[\frac{k-(N+1)}{2}\right] d. \tag{41}$$

Combining (40) and (41), we obtain

$$\exp\left[-j\psi_m(n) + jk_0 x_m \sin\theta(n)\right] \approx \exp\left[j\gamma(n)\left(m - \frac{(N+1)}{2}\right)\right]$$

where

$$\gamma(n) = k_0 d[\sin\theta(n) - \sin\theta(n-1)]. \tag{42}$$

Using the above equation, M in (35) can be rewritten as

$$M = -\exp\left[j\left(k - \frac{N+1}{2}\right)\gamma(n)\right] + \sum_{m=1}^{N} \exp\left[j\left(m - \frac{N+1}{2}\right)\gamma(n)\right]. \tag{43}$$

Using (43), X in (39) can be found

$$X = \exp\left[-jk\gamma(n)\right] \sum_{m=1}^{N} \exp[jm\gamma(n)] - 1. \tag{44}$$

The summation in (44) represents a geometric series, so it is equal to

$$\sum_{m=1}^{N} \exp[jm\gamma(n)] = \frac{\exp[j\gamma(n)] - \exp[j(N+1)\gamma(n)]}{1 - \exp[j\gamma(n)]}. \tag{45}$$

Using (45), X in (44) can be calculated as

$$X = \exp\left[j\left(\frac{N+1}{2} - k\right)\gamma(n)\right] \frac{\sin\left[\frac{N\gamma(n)}{2}\right]}{\sin\left[\frac{\gamma(n)}{2}\right]} - 1. \tag{46}$$

Thus, the imaginary part of X is

$$\Im[X] = \sin\left[\left(\frac{N+1}{2} - k\right)\gamma(n)\right] \frac{\sin\left[\frac{N\gamma(n)}{2}\right]}{\sin\left[\frac{\gamma(n)}{2}\right]}. \tag{47}$$

Finally, the kth component of the estimated gradient in (38) will be

$$\hat{g_k}(n) = 2\frac{\sin\delta_\psi}{\delta_\psi} \sin\left[\left(\frac{N+1}{2} - k\right)\gamma(n)\right] \frac{\sin\left[\frac{N\gamma(n)}{2}\right]}{\sin\left[\frac{\gamma(n)}{2}\right]} \tag{48}$$

ACKNOWLEDGMENT

The authors would like to thank Dr. K. Narimani and Mr. M. Hossu for helping with the test set-up.

REFERENCES

[1] G. Kefalas, "A phased-array ground terminal for satellite communications," *IEEE Trans. Commun.*, vol. 13, pp. 512–525, Dec. 1965.
[2] S. Taira, M. Tanaka, and S. Ohmori, "High gain airborne antenna for satellite communications," *IEEE Trans. Aerosp. Electron. Syst.*, vol. 27, no. 2, pp. 354–360, Mar. 1991.
[3] A. Zaghloul, O. Kilic, and E. Kohls, "System aspects and transmission impairments of active phased arrays for satellite communications," *IEEE Trans. Aerosp. Electron. Syst.*, vol. 43, pp. 176–186, Jan. 2007.
[4] R. Ersdal, G. Naerland, and O. Hakonsen, "A shipborne antenna for maritime satellite communications," *IEEE Trans. Commun.*, vol. 22, pp. 1310–1325, Sep. 1974.
[5] S. Durrani, "Maritime communications via satellites employing phased arrays," *IEEE Trans. Aerosp. Electron. Syst*, vol. 4, pp. 504–511, Jul. 1973.
[6] J. I. Alonso *et al.*, "Low cost electronically steered antenna and receiver system for mobile satellite communications," *IEEE Trans. Microw. Theory Tech.*, vol. 44, no. 12, pp. 2438–2449, 1996.
[7] D. Bodnar, B. Rainer, and Y. Rahmat-Samii, "A novel array antenna for MSAT applications," *IEEE Trans. Veh. Technol.*, vol. 38, pp. 86–94, 1989.
[8] Y. Ito and S. Yamazaki, "A mobile 12 GHz DBS television receiving system," *IEEE Trans. Broadcast.*, vol. 35, pp. 56–62, Mar. 1989.
[9] M. Fakharzadeh, S. Safavi-Naeini, S. H. Jamali, and P. Mousavi, "Zero-knowledge beamforming of phased array antennas based on simultaneous perturbation gradient approximation," in *Proc. IEEE Int. Symp. Antennas Propag.*, Albuquerque, NM, Jul. 2006, pp. 537–540.
[10] Y. Hwang, "Satellite antennas," *Proc. IEEE*, vol. 80, no. 1, pp. 183–193, Jan. 1992.
[11] S. Y. Eom *et al.*, "Design and test of a mobile antenna system with tri-band operation for broadband satellite communications and DBS reception," *IEEE Trans. Antennas Propag.*, vol. 55, pp. 3123–3133, Nov. 2007.
[12] Y. Bresler, V. Reddy, and T. Kailath, "Optimum beamforming for coherent signal and interferences," *IEEE Trans. Signal Process.*, vol. 36, no. 6, pp. 833–843, Jun. 1988.
[13] R. Miura, T. Tanaka, I. Chiba, A. Horie, and Y. Karasawa, "Beamforming experiment with a DBF multibeam antenna in a mobile satellite environment," *IEEE Trans. Antennas Propag.*, vol. 45, pp. 707–714, Apr. 1997.
[14] L. Godara and A. Cantoni, "Analysis of constrained LMS algorithm with application to adaptive beamforming using perturbation sequences," *IEEE Trans. Antennas Propag.*, vol. 34, pp. 368–379, Mar. 1986.
[15] L. C. Godara, "Application of antenna arrays to mobile communications, part ii: Beam-forming and direction of arrival considerations," *Proc. IEEE*, vol. 85, no. 8, pp. 1195–1254, Aug. 1997.
[16] D. Feldman and L. Griffiths, "A projection approach for robust adaptive beamforming," *IEEE Trans. Signal Process.*, vol. 42, no. 4, pp. 867–876, Apr. 1994.
[17] A. Swindlehurst and T. Kailath, "A performance analysis of subspace-based methods in the presence of model errors—Part 1: The music algorithm," *IEEE Trans. Signal Process.*, vol. 40, no. 7, pp. 1758–1774, Jul. 1992.
[18] S. Hayward, "Effects of motion on adaptive arrays," *IEE Proc. Radar, Sonar Navig.*, vol. 144, no. 1, pp. 15–20, Feb. 1997.
[19] B. Widrow and J. M. McCool, "A comparison of adaptive algorithms based on the methods of steepest descent and random search," *IEEE Trans. Antennas Propag.*, vol. 24, pp. 615–637, 1976.
[20] R. Davis, "Phase-only LMS and perturbation adaptive algorithms," *IEEE Trans. Aerosp. Electron. Syst.*, vol. 34, no. 1, pp. 169–178, 1998.
[21] A. Cantoni, "Application of orthogonal perturbation sequences to adaptive beamforming," *IEEE Trans. Antennas Propag.*, vol. 28, pp. 191–202, 1980.
[22] L. Godara, "Improved LMS algorithm for adaptive beamforming," *IEEE Trans. Antennas Propag.*, vol. 38, pp. 1631–1635, Oct. 1990.

[23] M. Fakharzadeh, P. Mousavi, S. Safavi-Naeini, and S. H. Jamali, "The effects of imbalanced phase shifters loss on phased array gain," *IEEE Antenna Wireless Propag. Lett.*, vol. 7, pp. 192–196, 2008.
[24] M. Fakharzadeh, "Optical and Microwave beamforming for phased array antennas," Ph.D. dissertation, Univ. Waterloo, Waterloo, ON, Canada, 2008.
[25] M. Fakharzadeh, S. H. Jamali, K. Narimani, P. Mousavi, S. Safavi-Naeini, and J. Ahmadi-Shokou, "Zero-knowledge beamforming for mobile satellite phased array antenna," presented at the 68th IEEE Veh. Technol. Conf. (VTC 2008), Calgary, AB, Canada, Sep. 2008.
[26] A. Bhattacharyya, *Phased Array Antenna: Floquet Analysis, Synthesis, BFNs and Active Array Systems*. New York: Wiley, 2006.
[27] P. Mousavi, M. Fakharzadeh, S. H. Jamali, K. Narimani, M. Hossu, H. Bolandhemmat, G. Rafi, and S. Safavi-Naeini, "A low-cost ultra low profile phased array system for mobile satellite reception using zero-knowledge beam-forming algorithm," *IEEE Trans. Antennas Propag.*, vol. 56, pp. 3667–3679, Dec. 2008.
[28] H. Bolandhemmat, M. Fakharzadeh, P. Mousavi, S. H. Jamali, and S. Safavi-Naeini, "Active stabilization of vehicle-mounted phased-array antennas," *IEEE Trans. Veh. Technol.*, to be published.

Mohammad Fakharzadeh (S'05–M'09) received the B.Sc. degree (honors) from Shiraz University, and the M.Sc. degree from Sharif University of Technology, Tehran, Iran, in 2000 and 2002, respectively, all in electrical engineering.

From 2004 to 2008, he was a Ph.D. student at the Intelligent Integrated Radio and Photonics Group, University of Waterloo, Waterloo, ON, Canada, where he is currently a Postdoctoral Researcher.

From January 2003 to September 2004, he was a faculty member in the Electrical Engineering Department, Chamran University of Ahvaz, Iran. Since June 2005, he has been a Consultant to the Intelwaves Technologies, developing the beamforming, signal processing and tracking algorithms for mobile satellite receiver phased array antennas. His areas of interest include: phased array design and beamforming, millimeter wave systems for short range wireless networks, miniaturized optical delay lines, and adaptive filters.

Mr. Fakharzadeh was the recipient of the University of Waterloo Outstanding Graduate Studies Award, 2008 Khwarizimi International Award, and the IEEE APS 2006 student paper finalist.

S. Hamidreza Jamali was born in Zanjan, Iran. He received the B.Sc. and M.Sc. degrees from the University of Tehran, Tehran, Iran, in 1978 and 1980, respectively, and the Ph.D. degree from Concordia University, Montreal, QC, Canada, in 1991.

From 1982 to 1983, he was with the Electronics Research and Production Center, a subsidiary of the Iran Broadcast Organization. In 1983, he joined the Department of Electrical and Computer Engineering, University of Tehran, where he is currently an Associate Professor. He also has been a Visiting Professor at the Electrical and Computer Engineering Department, University of Waterloo, Waterloo, ON, Canada and Intelwaves Technologies Chief Technical Officer, since November 2004. His current research interests include MIMO and smart antenna systems and the applications of coding and diversity techniques to wireless communications. He is the coauthor of a book entitled *Coded Modulation Techniques for Fading Channel* (New York: Kluwer Academic, 1994).

Pedram Mousavi (S'96–M'01) received the B.Sc. (Hons.) degree in telecommunication engineering from Iran University of Science and Technology, Tehran, in 1995 and the M.Sc. and Ph.D. degrees from University of Manitoba, Winnipeg, Canada, in 1997 and 2001, respectively, all in electrical engineering.

From 2001 to 2003, he was a Senior Microwave Engineer with Sirific Wireless Corp. where he worked on the development of multiband VCO for various wireless standards. From 2003 to 2004, he was a Postdoctoral Fellow with the Department of ECE and Centre for Integrated RF Engineering, University of Waterloo, conducting research on low cost low profile phased array antenna system for mobile satellite communication. Based on his research at the University of Waterloo he founded Intelwaves Technologies which he is currently the CEO. Intelwaves Technologies Ltd. is developing a comprehensive suite of intelligent antennas and radio systems that can be used to provide satellite TV programming and satellite broadband Internet access within moving vehicles, from passenger cars to commercial aircrafts. The company vision is to make car as a communication center. His research interest includes miniaturized intelligent antennas and radios, microwave and millimeter wave low profile/integrated adaptive antenna structures, and emerging technologies for microwave and millimeter wave in intelligent antennas.

Safieddin Safavi-Naeini received B.Sc. degree from the University of Tehran, Tehran, Iran, in 1974 and the M.Sc. and Ph.D. degrees from the University of Illinois at Urbana-Champaign, in 1975 and 1979, respectively, all in electrical engineering.

He joined the University of Waterloo, Waterloo, ON, Canada, in 1996 where he is now a Professor in the Department of Electrical and Computer Engineering and holds the RIM/NSERC Industrial Research Chair in Intelligent Radio/Antenna and Photonics. He has more than 30 years of research experience in antenna, RF/microwave technologies, integrated photonics, and computational electromagnetics. He has published more than 70 journal publications and 200 conference papers in international conferences. He has led several international collaborative research programs with research institutes in Germany (DAAD fund), Finland (Nokia), Japan, China (BVERI, Institute of Optics), and USA, which have resulted in novel technologies and efficient design methodologies. He has been scientific and technical consultant to many North American, European, and Asian international companies.